

Article

Assembly of Mn(III) Schiff Base Complexes with Heptacyanorhenate (IV)

Taisiya S. Sukhikh^{1,2} and Kira E. Vostrikova^{1,*} ¹ Nikolaev Institute of Inorganic Chemistry SB RAS, Novosibirsk 630090, Russia; sukhikh@niic.nsc.ru² Novosibirsk National Research State University, 630090 Novosibirsk, Russia

* Correspondence: vosk@niic.nsc.ru; Tel.: +7-383-316-5831

Received: 8 August 2017; Accepted: 29 August 2017; Published: 1 September 2017

Abstract: A pioneering research on a self-assembly of the magneto-anisotropic module $[\text{Re}(\text{CN})_7]^{3-}$ with the Mn(III) complexes involving *Salen* type (*N,N'*-ethylenebis(salicylideneimine)) Schiff base (SB) ligands was performed using the known $[\text{Mn}(\text{}^3\text{MeO}^-\text{Salen})(\text{H}_2\text{O})_2]_2(\text{ClO}_4)_2 \cdot \text{H}_2\text{O}$ (**1**) and the firstly synthesized $[\text{Mn}_2(\text{}^5\text{Me}^-\text{Salen})_2\text{OAc}]\text{PF}_6$ (**2**). In the case of **1**, a slow diffusion of the component solutions led to the ionic compound $\text{Ph}_4\text{P}[\text{Mn}(\text{}^3\text{MeO}^-\text{Salen})(\text{H}_2\text{O})_2]_2[\text{Re}(\text{CN})_7] \cdot 6\text{H}_2\text{O}$ (**3**). The direct mixing of the same solutions has resulted in the microcrystalline nearly insoluble solid $[\text{Mn}(\text{}^3\text{MeO}^-\text{Salen})(\text{H}_2\text{O})_4\text{Re}(\text{CN})_7]\text{ClO}_4 \cdot 1.5\text{MeCN} \cdot 6.5\text{H}_2\text{O}$, which is likely to comprise the pentanuclear clusters $[(\text{Mn}^{\text{III}}(\text{SB})(\text{H}_2\text{O}))_4\text{Re}(\text{CN})_7]^+$. The use of **2** resulted in a 2D-network assembly of octanuclear clusters, $[(\text{Mn}(\text{}^5\text{Me}^-\text{Salen}))_6(\text{H}_2\text{O})_2\text{Re}(\text{CN})_7]_2\text{Re}(\text{CN})_7\text{Cl}_2(\text{PF}_6) \cdot \text{H}_2\text{O}$ (**4**), incorporating one Re-center in a pentagonal bipyramid coordination environment, while another has strongly distorted capped trigonal prism as a coordination polyhedron. The latter was observed for the first time for Re(IV) complexes. A synthetic challenge to obtain the 0D assemblies with $\text{Re}:\text{Mn} \geq 3$ has yielded a hexanuclear complex $[\text{Mn}(\text{}^5\text{Me}^-\text{Salen})\text{H}_2\text{O}(i\text{-PrOH})][(\text{Mn}(\text{}^5\text{Me}^-\text{Salen}))_5\text{H}_2\text{O}(i\text{-PrOH})_2\text{Re}(\text{CN})_7](\text{PF}_6)_2(\text{OAc}) \cdot 2i\text{-PrOH}$ (**5**) being 1D chain via a bridging phenoxyl group. Owing to a low solubility of the final product, an addition of a bulk anion Ph_4B^- to the MeCN/MeOH solution of $[\text{Re}(\text{CN})_7]^{3-}$ and **1** in ratio 1:6 resulted in rhenium-free matter $[\text{Mn}(\text{}^3\text{MeO}^-\text{Salen})(\text{H}_2\text{O})_2][\text{Mn}(\text{}^3\text{MeO}^-\text{Salen})(\text{H}_2\text{O})\text{MeCN}](\text{Ph}_4\text{B})_2 \cdot 5\text{MeCN}$ (**6**).

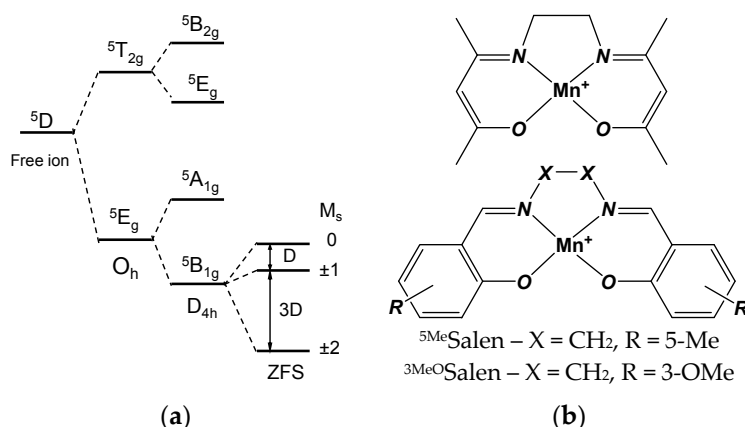
Keywords: Mn(III) Schiff base complexes; heptacyanorhenate; Re(IV); salen type ligands

1. Introduction

Complexes of Mn(III) with a quadridentate Schiff base (SB) ligand are widely used by chemists for applications in biology [1–4], catalysis [5–8], and molecular magnetism [9–15]. For a good reason, as many as eight Mn(III) ions of the twelve metallic centers are included in the first studied single-molecule magnet (SMM) $\text{Mn}_{12}\text{O}_{12}(\text{OA})_{16}(\text{H}_2\text{O})_4$ [16,17]. Along with a high spin state, the $\{\text{Mn}^{\text{III}}(\text{SB})\}$ magnetic modules possess uniaxial anisotropy upon completing their axial coordination positions during an assembly in heterometallic species. Why does this happen?

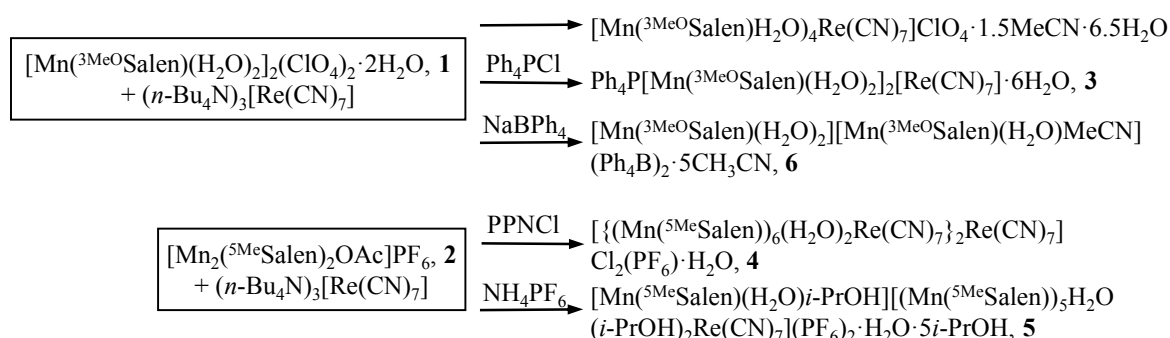
Mn(III) ion in the high-spin state with $S = 2$ ($3d^4$) is described by ${}^5\text{D}$ ground term. In an octahedral ligand field, the latter splits onto ${}^5\text{E}_g$ and ${}^5\text{T}_{2g}$ levels. Jahn–Teller (JT) distortion lowers the symmetry up to D_{4h} (tetragonal geometry), which leads to an additional splitting of ${}^5\text{E}_g$ into ${}^5\text{B}_{1g}$ and ${}^5\text{A}_{1g}$ and of ${}^5\text{T}_{2g}$ into ${}^5\text{E}_g$ and ${}^5\text{B}_{2g}$ (Scheme 1). Note that if the complex has an axially-elongated geometry (D_{4h}), the ground term is ${}^5\text{B}_{1g}$, while if the complex is compressed, ${}^5\text{A}_{1g}$ is the ground term. Further, the ground spin state degeneracy is removed by the second-order spin-orbit coupling (SOC)—called zero-field splitting (ZFS) (Scheme 1). Application of ZFS to ${}^5\text{B}_{1g}$ or ${}^5\text{A}_{1g}$ generates the lowest magnetization levels of $M_s = \pm 2$ or 0, with a gap of $4D$ between the ground spin state and the highest excited level. When ${}^5\text{B}_{1g}$ is the ground term, D is negative, and conversely, when ${}^5\text{A}_{1g}$ is the

ground term, D is positive with a Hamiltonian of $H = D(\hat{S}^2 - 1/3S(S + 1))$ [9]. It was shown in [18] that the anisotropy of the Mn^{III} depends greatly on JT distortion. In the case of axial elongation, the SB complexes exhibit a negative ZFS D parameter with finite uniaxial anisotropy [19].



Scheme 1. (a) Splitting of the 5D term by octahedral (O_h) and tetragonal (axial elongation, D_{4h}) fields and by zero-field splitting; (b) Quadridentate environment of $\text{Mn}(\text{III})$ by Schiff base ligands: *acacen* (top) or *salen* (N,N' -ethylene-bis(salicylideneimine)) (bottom), see text.

Thus, the Mn^{III} in the square planar $\{\text{NNOO}\}$ coordination environment of the SB ligand (Scheme 2) is an excellent building block for the construction of extended and molecular magnetic assemblies, because it possesses potentially vacant axial positions to bind heterometallic complex by means of ambidentate ligands. As a result of such coordination, a uniaxial magnetic anisotropy appears along the line of joint. Moreover, a wide variation of the SB ligand structure by means of the introduction of various substituents contributes to fine tailoring of target material organization, which is very important for the tuning of magnetic properties. Besides, it is sometimes necessary to take into consideration not only the choice of SB ligand but also the complete parameters of the $\text{Mn}(\text{III})$ precursor based on it. For example, it is essential to consider the presence or absence of dimerization in the manganese complex, as well as carefully select the counterions compensating the charge in both the starting materials and in the final products.



Scheme 2. The abridged synthetic protocols for the complexes under study.

In this report, we present a few examples showing how the choice of the starting compound incorporating the $\{\text{Mn}^{\text{III}}\text{SB}\}^+$ unit influences its assembly with $[\text{Re}(\text{CN})_7]^{3-}$ anion, as well as the structure and composition of the final product. Starting from the dimerized complex $[\text{Mn}(\text{}^3\text{MeOSalen})(\text{H}_2\text{O})_2]_2(\text{ClO}_4)_2 \cdot \text{H}_2\text{O}$ ($^3\text{MeOSalen} = N,N'$ -ethylene-bis(3-methoxysalicylideneimine)) (**1**) [20], an ionic compound $\text{Ph}_4\text{P}[\text{Mn}(\text{}^3\text{MeOSalen})(\text{H}_2\text{O})_2]_2[\text{Re}(\text{CN})_7] \cdot 6\text{H}_2\text{O}$ (**3**, Ph_4P^+ = tetraphenylphospho-

nium) was obtained. However, the introduction of the anion Ph_4B^- (tetraphenylborate) in the reaction mixture with the aim of making a heterometallic cation with maximal amount of $\{\text{Mn}^{\text{III}}\text{SB}\}^+$ units led to an anion exchange in **1**, giving a compound $[\text{Mn}(\text{}^3\text{MeO}\text{Salen})(\text{H}_2\text{O})_2][\text{Mn}(\text{}^3\text{MeO}\text{Salen})(\text{H}_2\text{O})\text{MeCN}](\text{Ph}_4\text{B})_2 \cdot 5\text{MeCN}$ (**6**) using diffusion technique. A rapid precipitation resulted in the microcrystalline material $[\text{Mn}(\text{}^3\text{MeO}\text{Salen})(\text{H}_2\text{O})_4\text{Re}(\text{CN})_7]\text{ClO}_4 \cdot 1.5\text{MeCN} \cdot 6.5\text{H}_2\text{O}$. A 2D complex network $[(\text{Mn}(\text{}^5\text{Me}\text{Salen}))_6(\text{H}_2\text{O})_2\text{Re}(\text{CN})_7]_2\text{Re}(\text{CN})_7\text{Cl}_2(\text{PF}_6) \cdot \text{H}_2\text{O}$ (**4**) and a 1D chain composed of hexanuclear moieties $[\text{Mn}(\text{}^5\text{Me}\text{Salen})(\text{H}_2\text{O})(i\text{-PrOH})][(\text{Mn}(\text{}^5\text{Me}\text{Salen}))_5\text{H}_2\text{O}(i\text{-PrOH})_2\text{Re}(\text{CN})_7](\text{PF}_6)_2(\text{MeCOO}) \cdot 2i\text{-PrOH}$ (**5**) were obtained when $[\text{Mn}_2(\text{}^5\text{Me}\text{Salen})_2\text{OAc}]\text{PF}_6$ (**2**, $\text{}^5\text{Me}\text{Salen} = N,N'$ -ethylenebis(5-methylsalicylideneimine), OAc = acetate) was used as a precursor (See Scheme 2).

2. Results and Discussion

2.1. Synthetic Approaches

Previously, we have studied heterometallic assemblies involving $\text{Mn}^{\text{III}}\text{SB}$ complexes and cyanometallates of *3d* [15,21], *4d* [22], and *5d* [14,23,24] metal ions. All of them were built on a $[\text{Mn}(\text{acacen})]^+$ (acacen = *N,N'*-ethylenebis(acetylacetonimine)) magnetic module. This comprehensive study has shown that in the case of diamagnetic $[\text{Fe}^{\text{II}}(\text{CN})_5\text{NO}]^{2-}$ metalloligand, the four compounds of different dimensionality were prepared depending on crystallization media [21]. Among them, two 0D assemblies, a trinuclear complex $[\{\text{Mn}(\text{acacen})\text{H}_2\text{O}\}_2\text{Fe}(\text{CN})_5\text{NO}] \text{EtOH}$ and an ionic compound with a pentanuclear bimetallic cation $[\{\text{Mn}(\text{acacen})\text{H}_2\text{O}\}_4\text{Fe}(\text{CN})_5\text{NO}][\text{Fe}(\text{CN})_5\text{NO}] 4\text{MeCN}$, one 1D coordination polymer $[\{\text{Mn}(\text{acacen})\}_2(i\text{-PrOH})\text{Fe}(\text{CN})_5\text{NO}]_n$, and two 2D networks $[\{\text{Mn}(\text{acacen})\}_2\text{M}(\text{CN})_5\text{NO}]_n$, $\text{M} = \text{Fe}^{\text{II}}, \text{Ru}^{\text{II}}$ [21,22]. A neutral 3D framework was not obtained due to non-bridging character of nitrosyl and only double negative charge of the metalloligand, as the formation of a 3D system is possible only in the case of the skeleton neutrality requiring three $\{\text{Mn}^{\text{III}}\text{SB}\}^+$ and one $[\text{M}(\text{CN})_{6+n}]^{3-}$. Owing to its structural versatility, the $[\text{Mn}^{\text{III}}\text{acacen}]^+$ synthon was chosen for the preparation of heterometallic coordination species involving homoleptic paramagnetic cyanometallates of different dimensionality. Inspired by a synthetic approach used in Ref. [25], we were able to synthesize the two anionic chain polymers involving paramagnetic octahedral hexacyanocomplexes as metalloligands, $\{(\text{Ph}_4\text{P})_2[\text{Mn}(\text{acacen})\text{M}(\text{CN})_6]\}_n$, $\text{M} = \text{Fe}^{\text{III}}, \text{Os}^{\text{III}}$ being single-chain magnets (SCMs) below 2.5 and 2.8 K, respectively [15,23]. However, all attempts to prepare low-dimensional (LD) assemblies incorporating $[\text{Mn}(\text{acacen})]^+$ and pentagonal bipyramidal (PB) geometry $[\text{Re}(\text{CN})_7]^{3-}$ failed. Highly magnetically anisotropic heptacyanorhenate(IV) is not commercially available, and may be prepared only as a tetrabutylammonium salt [26]. A combination of the latter with $[\text{Mn}(\text{acacen})]\text{Cl}$ —regardless of their ratio—led to the neutral 3D framework $\{[\{\text{Mn}(\text{acacen})\}_3\text{Re}(\text{CN})_7]\}_n$ that displays nontrivial strongly anisotropic magnetic behavior [14]. Interestingly, to the best of our knowledge, there are no other examples of the neutral 3D assembly incorporating a homoleptic cyanometallate and any $\{\text{Mn}^{\text{III}}\text{SB}\}$ complex. Only two-layered systems based on $[\text{Mn}^{\text{III}}\text{acacen}]^+$ and $[\text{M}(\text{CN})_{6+n}]^{3-}$ were reported earlier. One of them is $\{[\text{K}(18\text{-cr})(i\text{-PrOH})_2][\{\text{Mn}(\text{acacen})\}_2\text{Fe}(\text{CN})_6]\}_n$ (18-cr = 18-Crown-6-ether) [27], and the other— $\text{K}[\text{Mn}(\text{acacen})_2[\text{W}(\text{CN})_8] 2\text{H}_2\text{O}$ [28]. Based on the literature analysis, it could be concluded that with $\{\text{Mn}^{\text{III}}\text{SB}\}^+$ complexes of *salen*-type ligands the three manners of layered organization are possible. The first is based on the ratio of $\text{M}_{\text{CN}}:\text{Mn}^{\text{III}} = 1:2$. In this case, each manganese ion is surrounded by an equatorial SB and two axial nitrogen atoms from CN-groups of a cyanometallate unit, $[\text{M}^{\text{III}}(\text{CN})_{6+n}]^{3-}$, the four M–CN moieties of which coordinate to the Mn centers of $\{\text{Mn}(\text{SB})\}^+$ tectons, forming a 2D network having $[\text{CN}-\text{Mn}^{\text{III}}-\text{NC}-\text{M}-]_4$ cyclic repeating units. This arrangement was found for the three compounds involving orbitally degenerate hexacyanoferrate(III): $\text{K}[(\text{Mn}(\text{}^3\text{MeO}\text{salen}))_2\text{Fe}(\text{CN})_6] \cdot 2\text{DMF}$ [29], $\text{NEt}_4[(\text{Mn}(\text{}^5\text{-Cl}\text{Salen}))_2\text{Fe}(\text{CN})_6]$ ($\text{}^5\text{-Cl}\text{Salen} = N,N'$ -ethylenebis(5-chlorosalicylideneimine)) and $(\text{NEt}_4)[\{\text{Mn}(\text{salen})\}_2\text{Fe}(\text{CN})_6]$ [30–32]. The only example of second 2D network building fashion requiring the ratio of $\text{M}_{\text{CN}}:\text{Mn}^{\text{III}} = 1:4$ is $[(\text{Mn}(\text{saltmen}))_4\text{Fe}(\text{CN})_6]\text{ClO}_4 \cdot x\text{H}_2\text{O}$ (saltmen is

N,N'-(1,1,2,2-tetramethylethy-lene)bis(salicylideneimine)) [30]. In this assembly, iron and two *trans*-cyanide ligands are located on a four-fold rotation axis, and each of the four equatorial CN[−] groups are axially bonded to an Mn center of [Mn(saltmen)]⁺ cation, forming a four-petal vane unit (Mn–N_{CN} = 2.19(1) Å and Mn–N–C = 156.1(10)°). This pentanuclear cluster binds the four neighboring ones, forming dimers by interconnection of [Mn(saltmen)]⁺ complexes of the ligand phenoxy group, building a 2D network with [Mn–(O_{Ph})₂–Mn–NC–Fe–CN–]₄ repeat unit.

A neutral layering compound requiring the ratio of M_{CN}:Mn^{III} = 1:3 was obtained from [(Mn(³MeOSalen))₂(H₂O)₂](ClO₄)₂·2H₂O and K₃[Fe(CN)₆] [33]. The authors have attributed a 1D structure to the complex [(Mn(⁵MeSalen))₄(Mn(⁵MeSalen)H₂O)₂(Fe(CN)₆)₂]·MeCN·3H₂O, highlighting only a chain composed of the heptanuclear clusters [(MnSB)₆Fe(CN)₆]³⁺ connected with each other by a complex anion [Fe(CN)₆]^{3−}. However, two of the four equatorially bound by CN[−] to a central Fe center, {MnSB}⁺ units complete their coordination sphere by a phenoxy oxygen of the adjacent {MnSB}⁺ moiety joining the chains in a layer. Moreover, the two remaining {MnSB}⁺ units contain an axially coordinated H₂O molecule, which is involved in a hydrogen bonding with a related {MnSB(H₂O)}⁺ moiety from the neighboring layer linking them in 3D supramolecular system.

The majority of the already-investigated heterometallic systems incorporate the octahedral cyanometallates as a metalloligand. The assemblies involving octacyanometallates are less represented in literature, but they are numerous enough, while the complexes simultaneously including the Mn^{III}SB and heptacyano complexes are limited to the only studied compound, which is a 3D framework {[(Mn(acacen))₃Re(CN)₇]}_n [14]. It could be related to a high solubility of *n*-Bu₄NCl remaining in solution after the reaction and a small size of the *acacen*[−]. We have tried to prepare the LD assemblies involving [Re(CN)₇]^{3−} using the same cation metathesis employed in Ref. [34], where bis(triphenyl-phosphoranylidene)ammonium (PPN) cation was used to obtain trinuclear SMMs, PPN [(Mn^{III}salphenMeOH)₂M^{III}(CN)₆]·7MeOH (M = Fe, Ru, Os, H₂salphen = *N,N'*-bis(salicylidene)-1,2-diamino-benzene). However, an addition of PPNCl as a reactant to a solution of (*n*-Bu₄N)₃[Re(CN)₇] and [Mn(acacen)Cl] resulted in the formation of the 2D networks of PPN[(Mn(acacen))₂Re^{IV}(CN)₇]·Solv [35,36]. Additionally, [Mn(acacen)]⁺ form layered systems with [M(CN)₈]^{3−} (M = Mo, W) in the presence of PPN⁺ or Ph₄P⁺, respectively [37,38].

As the SMMs [11] and SCMs [9,39,40] based on octahedral homoleptic cyanometallates and *salen*-type {Mn^{III}SB}⁺ complexes were widely investigated previously, we would like to study the related assemblies involving PB [Re(CN)₇]^{3−} magnetic module with the aim of preparing new LD magnetic materials. For this purpose, complexes with two different SB ligands were selected.

One of them is [(Mn(³MeOSalen))₂(H₂O)₂](ClO₄)₂·2H₂O (1) [20], the second precursor involving (⁵MeSalen)^{2−} (see Scheme 1) was prepared by a modification of known method starting from [Mn^{III}₃O(OAc)₆]OAc [41,42], using NH₄PF₆ instead of NaClO₄. The crude product was recrystallized from acetonitrile, giving the crystals of compound [Mn₂(⁵MeSalen)OAc]PF₆ (2)—a tetramer with two types of anions: pentafluorophosphate and acetate. The crystal structure of 2 is discussed below.

The attempts to obtain 1D systems related to the chains {(Ph₄P)₂[Mn(acacen)M(CN)₆]}_n (M = Fe, Os) [15,23] starting from both precursors resulted in different complexes. In the case of 1, a slow diffusion of the components solutions led to an ionic compound Ph₄P[Mn(³MeOSalen)(H₂O)₂]₂[Re(CN)₇]·6H₂O (3), which was separated as the single crystals suitable for single crystal XRD (SCXRD). The direct mixing of the solutions resulted in the microcrystalline material [Mn(³MeOSalen)H₂O)₄Re(CN)₇](ClO₄)·1.5MeCN·6.5H₂O, which is likely to comprise the pentanuclear heterometallic clusters [(MnSB(H₂O))₄Re(CN)₇]⁺. This compound is almost insoluble in MeCN and alcohols, but decays into the constituents in hot water. The use of precursor 2 in the presence of PPNCl gave a 2D assembly {[(Mn(⁵MeSalen))₆(H₂O)₂Re(CN)₇]₂Re(CN)₇Cl₂·(PF₆)₂·H₂O} (4). A synthetic challenge for the molecular clusters with Re:Mn ≥ 3 has yielded a hexanuclear [Mn(⁵MeSalen)H₂O(*i*-PrOH)][(Mn(⁵MeSalen))₅H₂O(*i*-PrOH)₂Re(CN)₇](PF₆)₂(OAc)·2*i*-PrOH (5) species having one {MnSB}⁺ unit as a cation. An addition of the sodium salt of a bulk counter-ion Ph₄B[−] to the acetonitrile/methanol solution of the mixture of (*n*-Bu₄N)₃[Re(CN)₇] and 1 in ratio 1:6 resulted in

rhodium-free crystal material $[\text{Mn}(\text{}^3\text{MeO}^-\text{Salen})(\text{H}_2\text{O})_2][\text{Mn}(\text{}^3\text{MeO}^-\text{Salen})(\text{H}_2\text{O})\text{MeCN}](\text{Ph}_4\text{B})_2 \cdot 5\text{MeCN}$ (**6**). This certainly happened due to the low solubility of the latter.

2.2. Crystal Structure Description

The molecular and crystal structures of the studied compounds will be described in the order of their degree of complexity. First, homometallic precursors; then, heterometallic coordination compounds.

2.2.1. $[\text{Mn}(\text{}^5\text{Me}^-\text{Salen})_2\text{OAc}]\text{PF}_6$ (**2**)

An asymmetric unit of the compound **2** (Figure 1) is a dimer in which the $\{\text{Mn}(\text{SB})\}^+$ moieties are connected through a μ -acetate bridge in a *syn-anti* fashion. The 1D supramolecular organization is supported by the π - π interactions between SB ligands. The coordination polyhedron of each Mn ion is an axially elongated octahedron formed by two atoms O and two atoms N of the SB ligand in equatorial plane (mean distances Mn–O_{SB} of 1.8961(10) and Mn–N of 1.9842 Å), one atom O from acetate group (Mn–O of 2.1399(10) and 2.1064(11) Å), and one O atom of a neighboring $\{\text{MnSB}\}^+$. Such elongation is typical for $[\text{Mn}^{\text{III}}\text{SB}]^+$ complexes due to JT effect. Both independent Mn atoms form the short contacts Mn1–O21 of 2.3868(10), Mn1–Mn1 of 3.3822(4) Å, and Mn2–O21 of 2.8071(10), Mn2–Mn2 of 3.5304(4) Å binding the dimers in a chain (Table S1). These short distances are non-negligibly shorter compared to those for the related complex $[(\text{Mn}_2(\text{Salen})_2\text{OAc})\text{ClO}_4]$ [42]. According to the calculations [43], the π - π interactions with distances of 3.863 and 3.711 Å are present in **2** between the SB ligands coordinated to Mn1 and Mn2, respectively (Table S1).

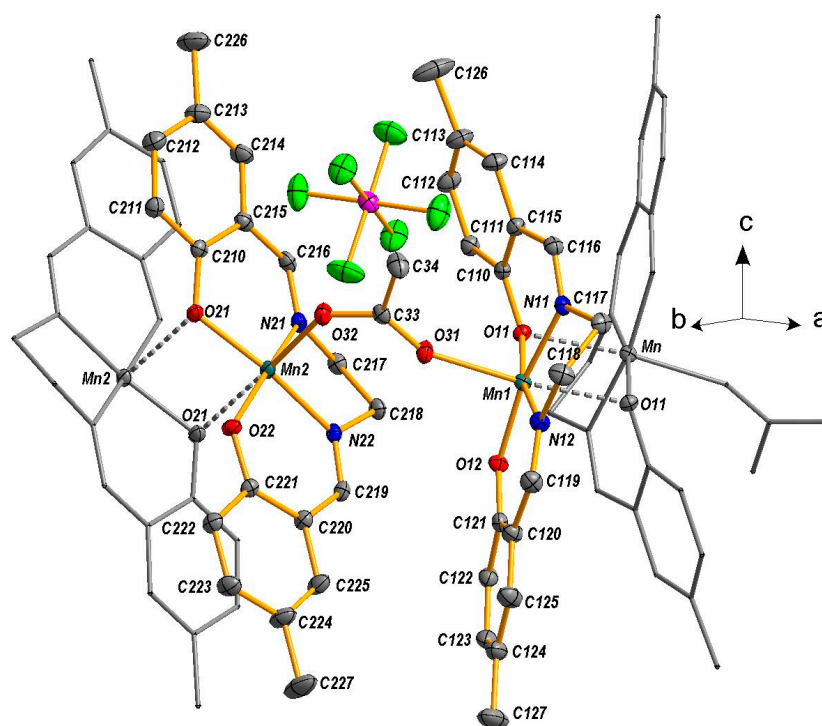


Figure 1. Asymmetric unit with numbering for **2**. The two $\{\text{Mn}(\text{SB})\}^+$ units manifold by symmetry are highlighted by grey color. Hydrogen atoms are omitted for clarity. SB: Schiff base.

2.2.2. $[\text{Mn}(\text{}^3\text{MeO}^-\text{Salen})(\text{H}_2\text{O})_2][\text{Mn}(\text{}^3\text{MeO}^-\text{Salen})(\text{H}_2\text{O})(\text{MeCN})](\text{Ph}_4\text{B})_2 \cdot 5\text{MeCN}$ (**6**)

The single crystals of **6** were obtained by a crystallization of the crude product from acetonitrile. The asymmetric unit involves six MeCN molecules, two anions Ph_4B^- , and two $[\text{MnSB}(\text{Solv})_2]^+$ units dimerized by hydrogen bonding (Figure 2a). If the coordination environment of Mn₂ in one molecule

is sufficiently symmetrical since the two aqua ligands located in apical positions complete square planar geometry of the central atom up to octahedral, then the Mn_1 complex contains one acetonitrile ligand in *trans* position of coordinated molecule of water. The inner dimer distances are close to those in **1** (see Table S1). However, due to the presence of MeCN ligand in coordination sphere of Mn_1 and hydrogen bonding of two other molecules of MeCN to an aqua ligand of Mn_2 , the dimer is not involved in propagated network of hydrogen bonds (unlike **1**). Moreover, the anions Ph_4B^- well separate binary $\{MnSB\}^+$ units from each other in crystal (Figure S1 in Supplementary Materials). Both ethylene carbons of $[Mn_1SB(H_2O)MeCN]^+$ are disordered over two positions. According to the calculations [43], there are no the π - π interactions between SB ligands in **6**.

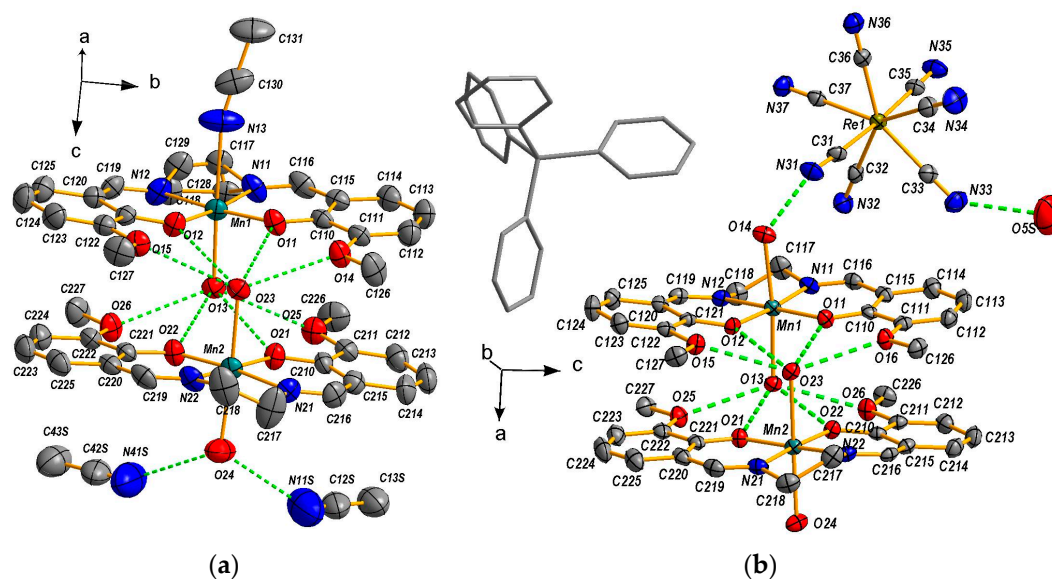


Figure 2. (a) Cationic dimer unit with numbering scheme for the compound **6**; (b) Asymmetric unit with numbering scheme for the compound **3**. The Ph_4B^- anion is tinted by a grey color. The green lines are hydrogen bonds. Hydrogen atoms and some solvent molecules are omitted for clarity.

2.2.3. $Ph_4P[Mn(3MeO\text{Salen})(H_2O)_2]_2[Re(CN)_7] \cdot 6H_2O$ (**3**)

The molecular and crystal structure of **3** is presented in Figure 2b. The asymmetric unit includes the two anions Ph_4B^- and $[Re(CN)_7]^{3-}$, as well as a pair of $[MnSB(H_2O)_2]^+$ moieties interconnected by hydrogen bonds between coordinated molecules of water and oxygen atoms of adjacent SB base ligand forming a dimer like in **1**. However, unlike the latter, despite of a shorter distance between the planes incorporating the chelating systems of $\{MnSB\}$ units (3.10 vs. 3.13 Å), according to the calculations [43], the π - π interactions between SB ligands are absent in **3**. The other feature of the structure is the chains formed of the dimers along *a* axis *via* hydrogen bonds between the aqua-ligands (Figure 3a). The crystal packing for **3** along the three axes is shown in Figure S2. According to the dihedral angles analysis (Table S2) [44,45], the coordination polyhedron of Re is a slightly distorted pentagonal bipyramid. The distance of $Re-C_{CN}$ varies in the range 2.099(4)–2.108(4) Å, which is comparable to that observed for $[Re(CN)_7]^{3-}$ in $(n-Bu_4N)_3[Re(CN)_7]$ (2.064(10)–2.123(11) Å) [26]. Five of the seven cyanide ligands of the $[Re(CN)_7]^{3-}$ anion are involved in hydrogen bonding with the two O atoms of SB and the three interstitial molecule of water (Figure 3b).

2.2.4. $[(Mn(5Me\text{Salen}))_6(H_2O)_2Re(CN)_7]_2Re(CN)_7Cl_2(PF_6) \cdot H_2O$ (**4**)

An asymmetric unit of **4** duplicated over the inversion center is shown in Figure 4. Due to its proximity to the inversion center (0.49 Å), one $[Re(CN)_7]^{3-}$ anion is disordered over two positions with the occupancy of 0.5. This connects two heptanuclear clusters $\{(Mn(5Me\text{Salen}))_6$

$(\text{H}_2\text{O})_2\text{Re}(\text{CN})_7$, in which a coordination polyhedron of Re2 has a coordination environment of distorted pentagonal bipyramid, while Re1 adopts a strongly distorted geometry which is difficult to ascribe to any seven-ligand coordination polyhedron family. However, it is closer to a capped trigonal prism rather than other polyhedra according to the dihedral angles analysis (Table S2) [44,45]. A formation of heptanuclear cluster $[\{\text{Mn}^{\text{III}}\text{SB}\}_6\text{M}(\text{CN})_n]^+$ was earlier reported only for heptacyanocomplexes [33,46,47].

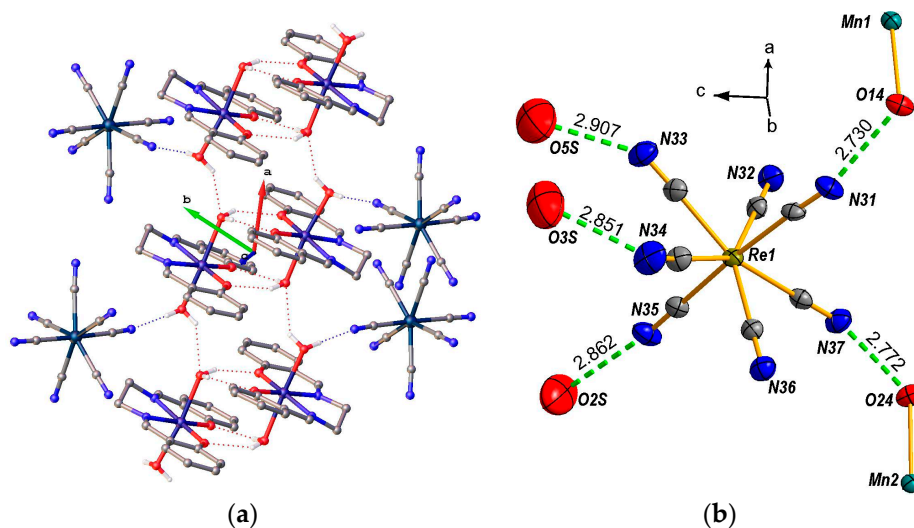


Figure 3. Hydrogen bonds in compound 3: (a) a supramolecular column composed of the $[\text{Mn}^{\text{III}}(\text{Salen}^{\text{MeO}})(\text{H}_2\text{O})_2]^+$ cations; (b) hydrogen bonds of the anion $[\text{Re}(\text{CN})_7]^{3-}$. Selected mean interatomic distances (Å) and angles (deg) for the complex: Re–C 2.104(4), C–N 1.1477(5), $\text{C}_{\text{eq}}\text{–Re–C}_{\text{eq}}$ 72.06(14), $\text{C}_{\text{ax}}\text{–Re–C}_{\text{eq}}$ 90.19(14), $\text{C}_{\text{ax}}\text{–Re–C}_{\text{ax}}$ 175.46(14), Re–C–N 178.2(4).

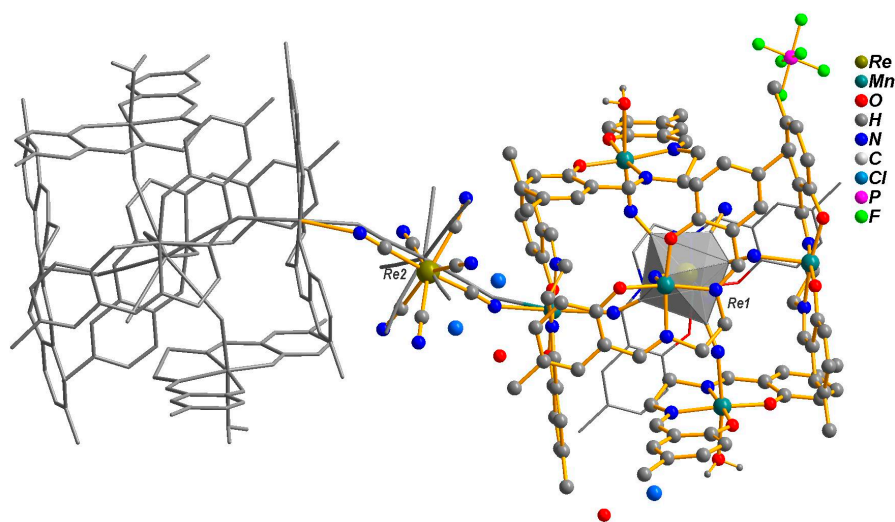


Figure 4. The asymmetric unit (ball-and-stick) of 4 duplicated over the inversion center. The disordered over two positions with occupancy 0.5 central anion $[\text{Re}(\text{CN})_7]^{3-}$ connects the two heptanuclear clusters $(\text{Mn}^{\text{III}}\text{Salen}^{\text{MeO}})_6(\text{H}_2\text{O})_2\text{Re}(\text{CN})_7$. Hydrogen atoms are omitted for clarity.

Assembly 4 is the first example of the coordination compound, where a heptacyanometallate binds the six $\{\text{Mn}^{\text{III}}\text{SB}\}^+$ units. Moreover, it is the first coordination compound incorporating a Re center with non-PB geometry of their coordination environment.

The six different Mn coordination polyhedra in **4** are depicted in Figure 4. The equatorial planes of the axially elongated octahedrons are composed of {OONN} atom set of SB ligand. The axial positions are occupied by N atoms of bridging CN-ligands and bridging O_{Ph} atom of neighboring SB ligand for Mn2–Mn4, aqua-ligand and CN group for Mn5 and Mn6. Mn1 are placed between the adjacent [Re(CN)₇]^{3−} anions. The coordination polyhedron of Mn4 can be attributed to an octahedron with a large margin, because of long distances Mn3–O42 and Mn4–O32 of 2.8574(53) and 2.7843(54) Å, respectively. However, according to the calculations [43], between the SB ligands coordinated to Mn3 and Mn4, the only π–π interaction with *d* = 3.804 Å was found in **4** (Table S1).

An analysis of the crystal packing has shown that the 2D assembly motif is realized in **4**. A layering structure is formed due to the formation of dimers involving Mn2–Mn2 and Mn3–Mn4 core (Figure 5, top and Figure S3). Hydrogen bonding between water molecules axially coordinated to Mn5 and Mn6 links the layers, forming a 3D supramolecular system.

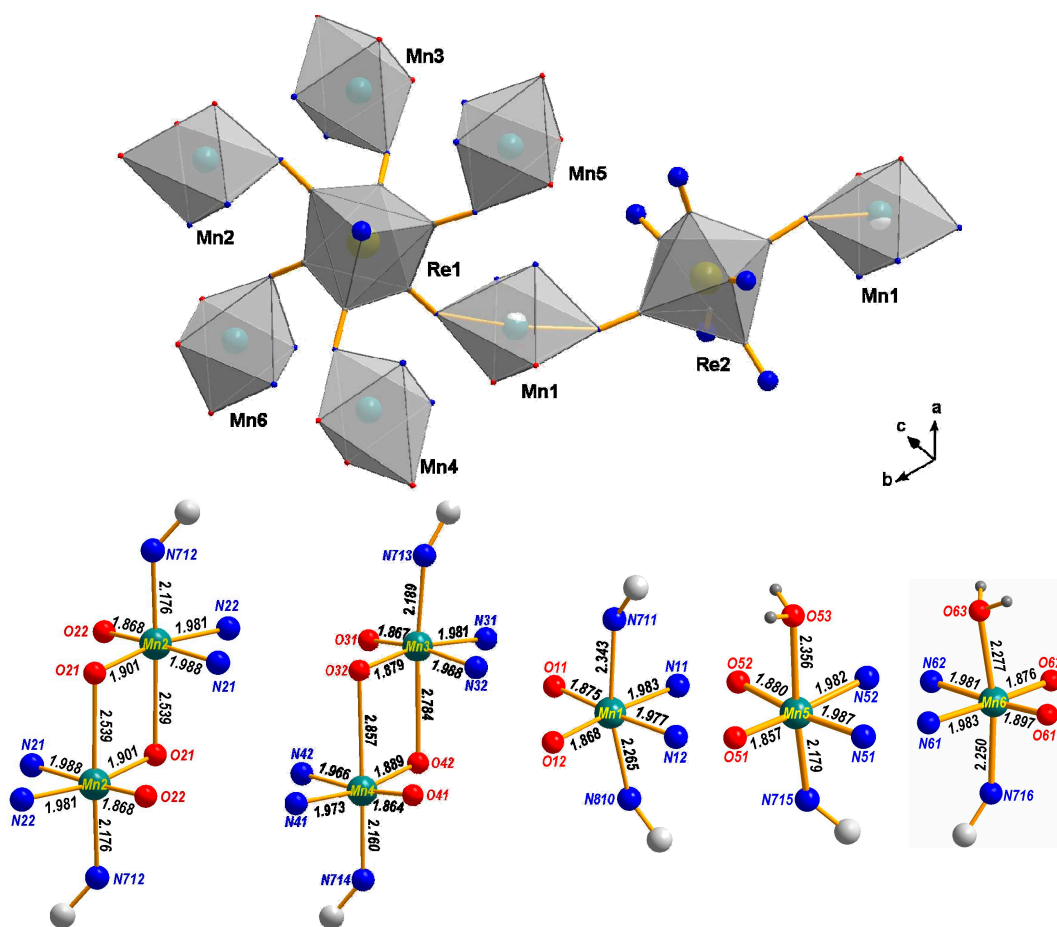


Figure 5. The coordination polyhedra in **4**. The equatorial planes of the axially elongated octahedrons are composed of {OONN} atom set of SB ligand.

A particular difficulty in the process of solving the structure was finding counterions, because for the total positive charge of +3 for the complex $[(\text{Mn}^{5\text{Me}}\text{Salen})_6(\text{H}_2\text{O})_2\text{Re}(\text{CN})_7]_2\text{Re}(\text{CN})_7]^{3+}$ at first was localized only one PF_6^- anion remaining from the precursor **2**. As mentioned above, the PPNCl was employed in the synthesis of **4**. Because the test for Cl^- using AgNO_3 was positive, compound **4** was analyzed for chlorine content, giving the two Cl^- per three Re^{IV} and twelve Mn^{III} .

2.2.5. $[\text{Mn}(\text{}^5\text{MeSalen})(\text{H}_2\text{O})i\text{-PrOH}][(\text{Mn}(\text{}^5\text{MeSalen}))_5\text{H}_2\text{O}(i\text{-PrOH})_2\text{Re}(\text{CN})_7](\text{PF}_6)_2(\text{OAc})\text{H}_2\text{O}(i\text{-PrOH})_2$ (5)

An asymmetric unit of **5** is presented in Figure 6. Unlike compound **4**, the structure of **5** involves the only crystallographically-independent Re center, which is incorporated in hexanuclear cluster $\{(\text{Mn}(\text{}^5\text{MeSalen}))_5\text{H}_2\text{O}(i\text{-PrOH})_2\text{Re}(\text{CN})_7\}$, in which coordination polyhedron of Re1 adopts PB geometry, which is strongly distorted in equatorial plane (see Table S2). The formation of an assembly $[\{\text{Mn}^{\text{III}}\text{SB}\}_6\text{M}(\text{CN})_n]^+$ was earlier reported only for octacyanomolibdate(IV) [48]. The sixth $\{\text{MnSB}\}$ unit represents a separate cation $[\text{Mn}(\text{}^5\text{MeSalen})\text{H}_2\text{O}(i\text{-PrOH})]^+$ connected to the $[\text{Re}(\text{CN})_7]^{3-}$ anion by a hydrogen bond formed between aqua-ligand and N atom of one of the cyanide groups (Figure 6). The six different Mn coordination polyhedra in **5** are depicted in Figure 7. The equatorial planes of the axially elongated octahedrons are composed of $\{\text{OONN}\}$ atom set of SB ligand in equatorial plane. The axial positions of $\{\text{MnSB}\}$ moieties are completed to octahedron by the atoms of O and/or N depending on the Mn center. Owing to a duplication over inversion center, the octahedrons involving Mn2 and Mn3 atoms linked by $\text{O}_{\text{Ph}}\text{-O}_{\text{Ph}}$ edge form the 1D assemblies in the crystal (Figure S4). According the calculations [43], the $\pi\text{-}\pi$ interaction with distances of 3.751 and 3.883 Å have been found in **5** between the SB ligands coordinated to Mn3 and Mn6, respectively (Table S1).

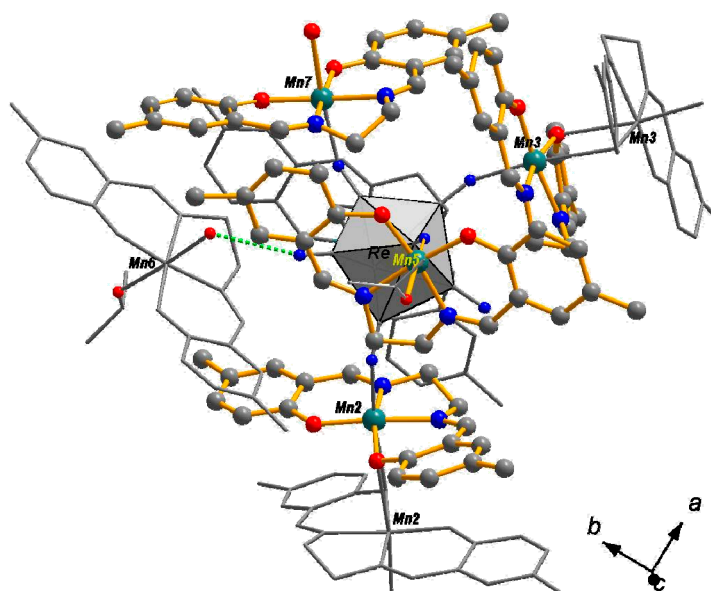


Figure 6. An asymmetric unit (ball-and-stick style) of **5** with Re polyhedron. The duplicated over the inversion center and back located $\{\text{MnSB}\}$ units as well as a hydrogen bound to $[\text{Re}(\text{CN})_7]^{3-}$ anion $[\text{MnSB}(\text{H}_2\text{O})i\text{-PrOH}]^+$ complex are painted in gray. Hydrogen atoms are omitted for clarity.

Unfortunately, the poor crystallinity of the compound **5** in solid state did not allow collection of diffraction data satisfying for the reliable localization of the solvent molecules and an anion. To fulfill the requirement of electroneutrality for $[\{\text{Mn}(\text{}^5\text{MeSalen})\text{H}_2\text{O}(i\text{-PrOH})][(\text{Mn}(\text{}^5\text{MeSalen}))_5\text{H}_2\text{O}(i\text{-PrOH})_2\text{Re}(\text{CN})_7]\}^{3+}$, three once-charged anions are needed. However, only two PF_6 were found based on the single-crystal XRD data. As a candidate for the third anion can be an acetate, which is structurally closed to *i*-PrOH molecule. Both have Y-like shape, only acetate is flat with rather short distances C–O, but, nevertheless, we did not dare to ascribe the acetate to any Mn atom, since the majority of the light atoms were refined isotropically and the anion could be delocalized between not only Mn coordination sites but also among the solvent locations. Additionally, based on IR spectra (Figure S4) it is not possible to ascribe with certainty any peak to the acetate vibrations against the background of SB-ligand frequencies intrinsic for heteroleptic complexes of Mn^{III} complexes involving SB and acetate [49]. Moreover, with a molecular weight exceeding 3000 g/mol for **5**, it is not possible

to distinguish the small difference between OAc^- and $i\text{-PrOH}$ based on elemental analysis. Certainly, a careful analysis of the magnetic data will be helpful in this case.

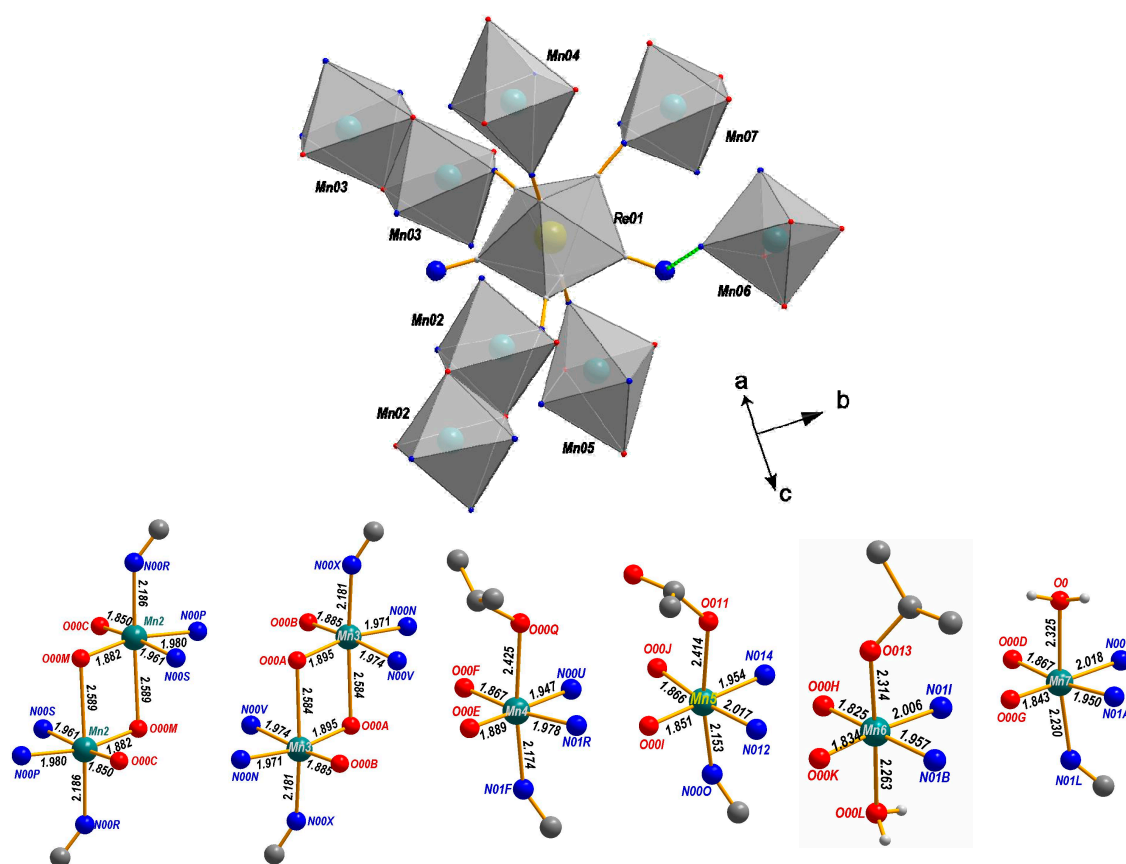


Figure 7. Coordination polyhedra in **5**. The equatorial planes of the axially elongated octahedrons are composed of {OONN} atom set of SB ligand. The duplicated Mn2 and Mn3 polyhedra show the direction of 1D assembly.

2.3. Crystal Structure Summary

Based on structural analysis and the chemistry performed, we can conclude that as in the case of heterometallic systems involving octahedral cyanide complexes of $3d$ metal ions, the assemblies incorporating $[\text{Re}(\text{CN})_7]^{3-}$ building block are characterized by a pronounced dimerization of the {Re–CN–Mn^{III}SB} moieties through a completion of their coordination environment to octahedral. This occurs because of a mutual coordination of phenoxyl groups of the SB ligand. The dimerization also takes place owing to hydrogen bonding of solvated units {Re–CN–Mn^{III}SB(ROH)} (where R = H or Alkyl). Formation in the solid state of discrete dimerized species of {SBMn^{III}...Mn^{III}SB} is favored by water. The greater the concentration of water in the reaction mixture, the higher the probability of the separated {Mn^{III}SB(H₂O)}₂ pairs formation instead of the joining *via* bridging CN[−] group of metalloligand. If the dimerization can be prevented using dry solvents, then a “coupling” through the coordination of phenolate oxygen requires the SB with a bulk connector –X–X– (Scheme 1b). A variation of the counterions along with a precise choice of the solvent media and crystallization techniques are of great importance. The design of LD assemblies involves an optimal combination of all abovementioned factors.

3. Conclusions

A pioneering research on the self-assembly of the strongly magneto-anisotropic module $[\text{Re}(\text{CN})_7]^{3-}$ with the Mn(III) complexes involving *Salen*-type Schiff base ligands was performed using previously known **1** and a new compound **2**. In the case of **1**, a slow diffusion of the component solutions led to an ionic compound **3**, separated as single crystals suitable for SCXRD. The direct mixing of the same solutions resulted in the microcrystalline material $[\text{Mn}^{3\text{MeO}}\text{Salen}(\text{H}_2\text{O})_4\text{Re}(\text{CN})_7]\text{ClO}_4 \cdot 1.5\text{MeCN} \cdot 6.5\text{H}_2\text{O}$, which is likely to comprise the pentanuclear clusters $[(\text{Mn}^{\text{III}}\text{SB}(\text{H}_2\text{O}))_4\text{Re}(\text{CN})_7]^+$. The use of **2**, with simultaneous addition of PPNCl, resulted in a 2D assembly **4** incorporating one Re center in pentagonal bipyramid coordination environment, while another has strongly distorted capped trigonal prism as a coordination polyhedron. The latter was observed for the first time among Re(IV) complexes. A trial to obtain 0D assemblies with $\text{Re}:\text{Mn} \geq 3$ has yielded a hexanuclear species **5** being a 1D chain via a bridging phenoxy group. Owing to a low solubility of the final product, an addition of a bulk anion Ph_4B^- to the MeCN/MeOH solution of $[\text{Re}(\text{CN})_7]^{3-}$ and **1** in ratio 1:6 resulted in rhenium-free material **6**. While compounds **2**, **3**, and **6** are not of interest as magnetic materials, the detailed magnetic investigations of complexes **4** and **5** are currently underway.

4. Experimental Section

All chemical reagents and solvents were purchased from commercial source and were used without further purification. The precursor $[(\text{Mn}^{3\text{MeO}}\text{Salen})_2(\text{H}_2\text{O})_2](\text{ClO}_4)_2 \cdot 2\text{H}_2\text{O}$ and the free ligands $\text{H}_2^{3\text{MeO}}\text{Salen}$, $\text{H}_2^{5\text{MeO}}\text{Salen}$ [20], as well as $(n\text{-Bu}_4\text{N})_3[\text{Re}(\text{CN})_7]$ [42] were prepared using published procedures. Elemental (C, H, N) analyses were carried out by standard methods with a Euro-Vector 3000 analyzer (Eurovector, Redavalle, Italy). Fourier transform infrared (FTIR) spectra were measured in KBr pellets with a NICOLET spectrophotometer (Thermo Electron Scientific Instruments LLC, Madison, WI, USA) in the $4000\text{--}375\text{ cm}^{-1}$ range.

4.1. Single-Crystal X-ray Diffraction

Single-crystal XRD data for **2**, **3**, **4** and **6** were collected by a Bruker Apex DUO diffractometer equipped with a 4K CCD area detector for **2**, **3**, **4** and **6** using the graphite-monochromated $\text{MoK}\alpha$ radiation and using $\text{CuK}\alpha$ radiation for **5** (Table 1). The ϕ - and ω -scan techniques were employed to measure intensities. Absorption corrections were applied with the use of the SADABS program [50]. The crystal structures were solved by direct methods and were refined by full-matrix least squares techniques by means of the *SHELXTL* package [51]. Atomic thermal displacement parameters for non-hydrogen atoms were refined anisotropically, except for some of the disordered solvent molecules. The positions of hydrogen atoms were calculated corresponding to their geometrical conditions and were refined using the riding model. Some hydrogen atoms of solvent molecules were not located due to their disorder. In the case of **5**, relatively poor crystals could only be grown which gave no detectable diffraction below a resolution d of 1.2 \AA . All efforts to harvest a crystal of better quality failed, and crystallization attempts were not successful.

Therefore, the data for **5** were collected using Cu source to increase the reflection intensities. Additionally, in the diffraction pattern, doubling the unit cell superstructural reflections were observed. Initially, a solution in the subcell ($C2/c$, $a' = 29.8872(8)$; $b' = 20.5181(8)$; $c' = 23.7390(7)\text{ \AA}$; $\beta = 93.368(3)^\circ$; $V = 14,532.3(8)\text{ \AA}^3$) gave the structure with the two $\{\text{MnSB}\}^+$ units disordered over two positions. Using the proper doubled unit cell eliminated this disorder, decreased mean I/σ from 14.6 to 9.4 at the same time. Along with the room temperature data collection, these factors have influenced the structure quality of **5** to be worse than the others. However, all atoms of the heterometallic assembly and even solvent molecules were located, although the light atoms could not be refined anisotropically.

Table 1. Crystallographic data for compounds 2–6.

Compound	2	6	3	4	5
Empirical formula	C ₃₈ H ₃₉ F ₆ Mn ₂ N ₄ O ₆ P	C ₉₆ H ₁₀₀ B ₂ Mn ₂ N ₁₀ O ₁₁	C ₆₇ H ₆₄ Mn ₂ N ₁₁ O ₁₈ PRE	C ₂₃₇ H ₂₂₄ Cl ₂ F ₆ Mn ₁₂ N ₄₅ O ₃₀ PRE ₃	C ₁₃₃ H ₁₆₀ F ₁₂ Mn ₆ N ₁₉ O ₂₀ P ₂ Re
CCDC number*	1567008	1567011	1567010	1567009	1567012
Formula weight	902.58	1701.35	1638.34	5616.35	3150.57
Crystal system	triclinic	monoclinic	triclinic	triclinic	monoclinic
SG	<i>P</i> -1	<i>P</i> ₂ ₁ / <i>c</i>	<i>P</i> -1	<i>P</i> -1	<i>P</i> ₂ ₁ / <i>n</i>
Unit cell <i>a</i> , Å	11.3880(4)	15.9891(18)	14.2002(9)	13.8130(3)	23.7380(7)
<i>b</i> , Å	11.8845(4)	27.544(3)	15.7993(9)	15.0609(3)	20.5122(6)
<i>c</i> , Å	15.3829(5)	21.779(2)	18.0470(11)	30.1361(7)	29.8804(9)
α (°)	75.0794(12)		84.638(3)	94.4470(10)	
β (°)	75.9749(13)	108.762(4)	82.694(4)	93.2230(10)	93.370(2)
γ (°)	84.3937(13)		65.057(3)	94.1440(10)	
<i>V</i> , Å ³	1950.38(12)	9081.7(17)	3637.9(4)	6222.1(2)	14524.2(7)
<i>Z</i>	2	4	2	1	4
<i>d</i> _{calc.} , g/cm ³	1.537	1.244	1.496	1.499	1.437
<i>T</i> , (°)	150(2)	200(2)	200(2)	200(2)	298
<i>F</i> (000)	924	3576	1654	2829	6424
Absorption coef., mm ⁻¹	0.768	0.342	2.098	2.143	6.609
Crystal size, mm ³	0.30 × 0.15 × 0.03	0.33 × 0.08 × 0.08	0.30 × 0.15 × 0.13	0.24 × 0.1 × 0.04	0.17 × 0.17 × 0.13
2θ _{max} (°)	59.48	50.05	57.8	50.16	80.6
Index range	−15 ≤ <i>h</i> ≤ 15 −14 ≤ <i>k</i> ≤ 16 −21 ≤ <i>l</i> ≤ 21	−19 ≤ <i>h</i> ≤ 19 −32 ≤ <i>k</i> ≤ 32 −25 ≤ <i>l</i> ≤ 25	−19 ≤ <i>h</i> ≤ 19 −21 ≤ <i>k</i> ≤ 21 −24 ≤ <i>l</i> ≤ 24	−19 ≤ <i>h</i> ≤ 19 −21 ≤ <i>k</i> ≤ 21 −24 ≤ <i>l</i> ≤ 24	−19 ≤ <i>h</i> ≤ 16 −11 ≤ <i>k</i> ≤ 17 −24 ≤ <i>l</i> ≤ 25
Reflections: collected	27,193	125,931	43,543	53,423	41,496
independent	10,872	16,018	18,851	22,053	8642
<i>I</i> ≥ 2σ(<i>I</i>)	9134	9349	16,297	13,745	5302
Parameters	520	1143	909	1593	1053
Completeness, %	97.7	100	98.5	99.7	96.2
GoF	1.022	1.021	1.120	0.978	1.075
Fin. <i>R</i> indices (<i>I</i> > 2σ(<i>I</i>))	R1 = 0.0319, wR2 = 0.0780	R1 = 0.0563, wR2 = 0.1282	R1 = 0.0394, wR2 = 0.0944	R1 = 0.0570, wR2 = 0.1131	R1 = 0.1082, wR2 = 0.1959
Δ _{max} , Δ _{min} , (e Å ⁻³)	−0.417, 0.422	−0.336, 0.707	−0.784, 2.182	−1.186, 1.416	−0.646, 0.871

* Further details may be obtained from the Cambridge Crystallographic Data Centre on quoting the depository numbers 1567008–1567012 (<http://www.ccdc.cam.ac.uk>).

4.2. Synthetic Details

4.2.1. Synthesis of Complex 2, [(Mn^{5Me}Salen)₂(OAc)]PF₆

To a stirred solution of the ligand H₂(^{5Me}Salen) (0.80 g, 2.7 mmol) in MeOH (100 mL) NaOH (0.216 g, 5.4 mmol) was added with cooling. This solution was added dropwise to a solution of [Mn^{III}₃O(OAc)₆]OAc (0.63 g, 0.9 mmol) in methanol (100 mL), and then NH₄PF₆ (0.652 g, 4 mmol) was added to the reaction mixture. The latter was stirred for 48 h at room temperature. The solvent was evaporated under reduced pressure. The crude solid was recrystallized from acetonitrile. Yield: 0.79 g, 65%. C₃₈H₃₉F₆Mn₂N₄O₆P (902.58) calcd. C 50.57, H 4.36, N 6.21; found C 50.43, H 4.4, N 6.22. IR:ν = 3459.6, 3015.6, 2925.5, 1638.7, 1625.4, 1550.9, 1541.2, 1468.0, 1440.6, 1415.9, 1380.1, 1344.4, 1339.6,

1325.6, 1297.5, 1276.4, 1261.4, 1249.3, 1221.9, 1201.6, 1165.1, 1141.9, 1090.2, 1047.3, 1010.7, 979.3, 976.0, 958.6, 945.1, 878.1, 845.8, 802.6, 775.6, 741.5, 638.8, 616.2, 557.9, 481.5, 460.4 cm⁻¹, Figures S4 and S5.

4.2.2. Synthesis of Complex 3, Ph₄P[Mn(³MeO-Salen)(H₂O)₂]₂[Re(CN)₇]-6H₂O

To a hot solution of **1** (27 mg, 0.025 mmol) in a mixture of H₂O/MeCN (3/2, 5 mL) Ph₄PCl (60 mg, 0.16 mmol) was added. After cooling the solution to room temperature, a white precipitate of Ph₄PClO₄ was removed, and the filtrate was divided equally between the three narrow (diameter 5 mm) glass tubes. A buffer layer of the solvent mixture (H₂O/MeCN, 1/3, 4 mL) divided in three portions was carefully placed on a filtrate layer, on the latter, in turn, a layer of (*n*-Bu₄N)₃[Re(CN)₇] solution (54 mg, 0.05 mmol) in MeCN (3 mL) divided into three portions, were placed on the top. The tubes were stopped with parafilm and left undisturbed during one month in the dark until the microcrystalline reddish-brown powder was formed. After separation of this solid, a filtrate was still colored in brown. The mother liquor was allowed to evaporate slowly. After one week, the elongated block-shaped dichroic brown-green crystals of **3** had formed. Yield: 11 mg, 27%. C₆₇H₆₄Mn₂N₁₁O₁₈PRE (1638.34) calcd. C 42.34, H 4.49, N 18.88; found C 42.54, H 4.53, N 19.00. IR: see Figures S6 and S7.

The crystals of the microcrystalline reddish-brown sample were too small to be studied by SCXRD. The formula [Mn(³MeO-Salen)H₂O)₄Re(CN)₇][ClO₄·1.5MeCN·6.5H₂O] (2243.66) based on C, H, N analysis and IR spectra. calcd. C 43.90, H 4.38, N 10.30; found C 43.95, H 4.2, N 10.4. IR: Figure S8.

4.2.3. Synthesis of Complex 4, [(Mn⁵MeSalen)₆(H₂O)₂Re(CN)₇]₂Re(CN)₇Cl₂·PF₆·H₂O

To a hot solution of **2** (20 mg, 0.02 mmol) in MeOH/EtOH (3/1, 2 mL) a solution of PPNCl (66 mg, 0.115 mmol) and (*n*-Bu₄N)₃[Re(CN)₇] (42 mg, 0.038 mmol) in MeOH (2 mL) was added. The mixture was stirred for 10 min and cooled to room temperature. A white precipitate was removed and *i*-PrOH (1 mL) was added to the filtrate. A vial with the reaction mixture was capped by a perforated top and left undisturbed in the dark for a week. The dark crystals were collected by suction filtration. Yield: 10.5 mg, 57%. C₂₃₇H₂₃₃Cl₂F₆Mn₁₂N₄₅O₃₃PRE₃ (5616.35) calcd. C 50.17, H 4.14, N 11.12; found C 50.9, H 4.5, N 10.75. As some white powder impurities were in the sample, the analysis fit better considering the formula 4·(PPNPF₆)_{0.1} (5766.84) calcd. C 50.73, H 4.21, N 10.95, Cl 1.23; found C 50.9, H 4.5, N 10.75, Cl 1.2. IR: see Figure S5.

4.2.4. [Mn(⁵MeSalen)H₂O(*i*-PrOH)][(Mn(⁵MeSalen))₅H₂O(*i*-PrOH)₂Re(CN)₇](PF₆)₂(OAc)·2*i*-PrOH, **5**

To a solution of **2** (20 mg, 0.019 mmol) in MeOH (3 mL), NH₄PF₆ (14 mg, 0.056 mmol) was added on stirring. Some insoluble solid was removed by filtration. A solution of (*n*-Bu₄N)₃[Re(CN)₇] (14 mg, 0.0128 mmol) in MeOH (1 mL) was added to a stirred filtrate. *i*-PrOH (1 mL) was added to the reaction mixture. A vial capped with a perforated top was kept in the dark for three days. The dark cube-shape crystals were collected by suction filtration. Yield: 12 mg, 60%. C₁₃₃H₁₆₀F₁₂Mn₆N₁₉O₂₀P₂Re (3150.57) calcd. C 50.70, H 5.12, N 8.45; found C 50.4, H 4.9, N 8.4. IR: see Figure S4.

4.2.5. Synthesis of Complex 6, [Mn(³MeO-Salen)(H₂O)₂][Mn(³MeO-Salen)(H₂O)MeCN](Ph₄B)₂·5MeCN

When a solution of *n*-Bu₄NBPh₄ (131 mg, 0.233 mmol) in MeCN (3 mL) was added to a solution (MeCN, 5 mL) containing **2** (60 mg, 0.057 mmol) and (*n*-Bu₄N)₃[Re(CN)₇] (42 mg, 0.038 mmol), a microcrystalline dark powder immediately precipitated. The latter was filtered and recrystallized from hot acetonitrile. The crystals formed overnight were collected by suction filtration, rinsed by dichloromethane, and air-dried. Yield: 20 mg, 20.5%. C₉₆H₁₀₀B₂Mn₂N₁₀O₁₁ (1701.35) calcd. C 67.77, H 5.92, N 8.23; found C 67.9, H 6.0, N 8.3. IR: see Figures S9 and S10.

Supplementary Materials: The following are available online at www.mdpi.com/2304-6740/5/3/59/s1. Cif and cif-checked files. Table S1. Some geometric parameters related to the contacts of the adjacent [MnSB]⁺ or [MnSB(Solv)_n]⁺ units. Figure S1. The crystal packing in the compound **6**. View along the axis *c* (left) and *a* (right). Hydrogen atoms are omitted. Figure S2. The crystal packing in the compound **6**. View along the three axes. Hydrogen atoms are omitted. Figure S3. Schematic presentation of a layer in **4**. SB ligand is reduced

for clarity. Table S2. Ideal and observed angles for the complex anion $[\text{Re}(\text{CN})_7]^{3-}$. Figure S4. IR spectra of the compound 5 and its precursor 2 registered in KBr pellets. Figure S5. IR spectra of the compound 4 and its precursor 2 registered in KBr pellets. Figure S6. IR spectra of the compound 3 and its precursor 1 registered in KBr pellets. Figure S7. IR spectra of the compound 3 and Ph_4PCl . Figure S8. IR spectra of the compound 3 and $[\text{Mn}^{3\text{MeO}}\text{SalenH}_2\text{O}]_4\text{Re}(\text{CN})_7[\text{ClO}_4 \cdot 1.5\text{MeCN} \cdot 6.5\text{H}_2\text{O}]$ in KBr pellets. Figure S9. IR spectra of the compound 6 and its precursor 1 registered in KBr pellets. Figure S10. IR spectra of the compound 6 and NaPh_4B registered in KBr pellets. Table S3. Selected bond lengths (Å) and angles (deg.) for $\{\text{Re}(\text{CN})_7\}$ units.

Acknowledgments: This work was supported in part by European Commission (PIIFR-GA-2011-911689) and the Russian Foundation for Basic Research under grant number 16-03-00880-a.

Author Contributions: Kira E. Vostrikova conceived, designed, and performed the chemical experiment, as well as wrote the paper; Taisiya S. Sukhikh performed a crystallographic study and participated in the article editing.

Conflicts of Interest: The authors declare no conflict of interest.

References

1. Liu, Q.R.; Xue, L.W.; Zhao, G.Q. Manganese(III) complexes derived from bis-Schiff Bases: Synthesis, structures, and antimicrobial activity. *Rus. J. Coord. Chem.* **2014**, *40*, 757–763. [[CrossRef](#)]
2. Kumar, G.; Kumar, D.; Singh, C.P.; Kumar, A.; Rana, V.B. Synthesis, physical characterization and antimicrobial activity of trivalent metal Schiff base complexes. *J. Serb. Chem. Soc.* **2010**, *75*, 629–637. [[CrossRef](#)]
3. Singh, D.P.; Kumar, K.; Sharma, C.; Aneja, K.R. Template synthesis, spectroscopic, antibacterial, and antifungal studies of trivalent transition metal ion macrocyclic complexes. *J. Enzyme Inhib. Med. Chem.* **2010**, *25*, 544–550. [[CrossRef](#)] [[PubMed](#)]
4. Surati, K.R. Synthesis, spectroscopy and biological investigations of manganese(III) Schiff base complexes derived from heterocyclic beta-diketone with various primary amine and 2,2'-bipyridyl. *Spectrochim. Acta Part A-Mol. Biomol. Spectrosc.* **2011**, *79*, 272–277. [[CrossRef](#)] [[PubMed](#)]
5. Signorella, S.; Hureau, C. Bioinspired functional mimics of the manganese catalases. *Coord. Chem. Rev.* **2012**, *256*, 1229–1245. [[CrossRef](#)]
6. Baleizao, C.; Garcia, H. Chiral salen complexes: An overview to recoverable and reusable homogeneous and heterogeneous catalysts. *Chem. Rev.* **2006**, *106*, 3987–4043. [[CrossRef](#)] [[PubMed](#)]
7. Gupta, K.C.; Sutar, A.K.; Lin, C.-C. Polymer-supported Schiff base complexes in oxidation reactions. *Coord. Chem. Rev.* **2009**, *253*, 1926–1946. [[CrossRef](#)]
8. Cozzi, P.G. Metal–Salen Schiff base complexes in catalysis: Practical aspects. *Chem. Soc. Rev.* **2004**, *33*, 410–421. [[CrossRef](#)] [[PubMed](#)]
9. Miyasaka, H.; Saitoh, A.; Abec, S. Magnetic assemblies based on Mn(III) salen analogues. *Coord. Chem. Rev.* **2007**, *251*, 2622–2664. [[CrossRef](#)]
10. Kachi-Terajima, C.; Mori, E.; Eiba, T.; Saito, T.; Kanadani, C.; Kitazawa, T.; Miyasaka, H. Mn^{III} Salen-type single-molecule magnet fixed in a two-dimensional network. *Chem. Lett.* **2010**, *39*, 94–95. [[CrossRef](#)]
11. Pedersen, K.S.; Bendix, J.; Clérac, R. Single-molecule magnet engineering: Building block approaches. *Chem. Commun.* **2014**, *50*, 4396–4415. [[CrossRef](#)] [[PubMed](#)]
12. Clemente-León, M.; Coronado, E.; López-Jordà, M. 2D, 3D bimetallic oxalate-based ferromagnets prepared by insertion of Mn^{III} -salen type complexes. *Dalton Trans.* **2013**, *42*, 5100–5110. [[CrossRef](#)] [[PubMed](#)]
13. Yoon, J.H.; Lim, K.S.; Ryu, D.W.; Lee, W.R.; Yoon, S.W.; Suh, B.J.; Hong, C.S. Synthesis, crystal structures, and magnetic properties of cyanide-bridged $\text{W}^{\text{V}}\text{Mn}^{\text{III}}$ anionic coordination polymers containing divalent cationic moieties: Slow magnetic relaxations and spin crossover phenomenon. *Inorg. Chem.* **2014**, *53*, 10437–10442. [[CrossRef](#)] [[PubMed](#)]
14. Samsonenko, D.G.; Paulsen, C.; Lhotel, E.; Mironov, V.S.; Vostrikova, K.E. $[\text{Mn}^{\text{III}}(\text{Schiff base})_3[\text{Re}^{\text{IV}}(\text{CN})_7]]$, highly anisotropic 3D coordination framework: Synthesis, crystal structure, magnetic investigations, and theoretical analysis. *Inorg. Chem.* **2014**, *53*, 10217–10231. [[CrossRef](#)] [[PubMed](#)]
15. Rams, M.; Peresyphkina, E.V.; Mironov, V.S.; Wernsdorfer, W.; Vostrikova, K.E. Magnetic Relaxation of 1D Coordination Polymers $(\text{X})_2[\text{Mn}(\text{acacen})\text{Fe}(\text{CN})_6]$, $\text{X} = \text{Ph}_4\text{P}^+$, Et_4N^+ . *Inorg. Chem.* **2014**, *53*, 10291–10300. [[CrossRef](#)] [[PubMed](#)]

16. Caneschi, A.; Gatteschi, D.; Sessoli, R.; Barra, A.L.; Brunel, L.C.; Guillot, M. Alternating current susceptibility, high field magnetization, and millimeter band EPR evidence for a ground $S = 10$ state in $[\text{Mn}_{12}\text{O}_{12}(\text{CH}_3\text{COO})_{16}(\text{H}_2\text{O})_4] \cdot 2\text{CH}_3\text{COOH} \cdot 4\text{H}_2\text{O}$. *J. Am. Chem. Soc.* **1991**, *113*, 5873–5874. [[CrossRef](#)]
17. Lis, T. Preparation, structure, and magnetic properties of a dodecanuclear mixed-valence manganese carboxylate. *Acta Crystallogr. Sect. B.* **1980**, *36*, 2042–2046. [[CrossRef](#)]
18. Gerritsen, H.J.; Sabinsky, E.S. Paramagnetic Resonance of Trivalent Manganese in Rutile (TiO_2). *Phys. Rev.* **1963**, *132*, 1507–1512. [[CrossRef](#)]
19. Kennedy, B.J.; Murray, K.S. Magnetic properties and zero-field splitting in high-spin Mn(III) complexes. 1. Mononuclear and polynuclear Schiff-base chelates. *Inorg. Chem.* **1985**, *24*, 1552–1557. [[CrossRef](#)]
20. Zhang, C.-G.; Tian, G.-H.; Ma, Z.-F.; Yan, D.-Y. Synthesis, crystal structure and properties of a novel di- μ_2 -aqua bridged binuclear manganese(III) Schiff base complex $[\text{Mn}(\text{vanen})(\text{H}_2\text{O})_2]_2(\text{ClO}_4)_2 \cdot 2\text{H}_2\text{O}$. *Trans. Met. Chem.* **2000**, *25*, 270–273. [[CrossRef](#)]
21. Peresyphkina, E.V.; Vostrikova, K.E. $2[\text{Mn}(\text{acacen})]^+ + 1[\text{Fe}(\text{CN})_5\text{NO}]_2^-$ polynuclear heterobimetallic coordination compounds of different dimensionality in the solid state. *Dalton Trans.* **2012**, *41*, 4100–4106. [[CrossRef](#)] [[PubMed](#)]
22. Peresyphkina, E.V.; Samsonenko, D.G.; Vostrikova, K.E. Heterobimetallic coordination polymers involving 3d metal complexes and heavier transition metals cyanometallates. *J. Solid State Chem.* **2015**, *224*, 107–114. [[CrossRef](#)]
23. Peresyphkina, E.V.; Majcher, A.; Rams, M.; Vostrikova, K.E. A single chain magnet involving hexacyanoosmate. *Chem. Commun.* **2014**, *50*, 7150–7153. [[CrossRef](#)] [[PubMed](#)]
24. Vostrikova, K.E. Homoleptic Osmium Cyanide Complexes: Synthesis and Perspective Application in Molecular Magnetism. In *Osmium: Synthesis Characterization and Applications*; Wise, G., Ed.; Nova Science Publishers: New York, NY, USA, 2015; pp. 43–78. ISBN 978-1-63483-517-6.
25. Re, N.; Gallo, E.; Floriani, C.; Miyasaka, H.; Matsumoto, N. Magnetic properties of a one-dimensional ferromagnet containing a Mn(III)–NC–Fe(III) linkage: Synthesis and crystal structure of a chainlike $[\text{Mn}(\text{acacen})\text{Fe}(\text{CN})_6]_n^{2n-}$ -polyanion. *Inorg. Chem.* **1996**, *35*, 6004–6008. [[CrossRef](#)]
26. Bennett, M.V.; Long, J.R. New Cyanometalate Building Units: Synthesis and Characterization of $[\text{Re}(\text{CN})_7]^{3-}$ and $[\text{Re}(\text{CN})_8]^{3-}$. *J. Am. Chem. Soc.* **2003**, *125*, 2394–2395. [[CrossRef](#)] [[PubMed](#)]
27. Miyasaka, H.; Okawa, H.; Miyazaki, A.; Enoki, T. Synthesis, crystal and network structures, and magnetic properties of a hybrid compound: $[\text{K}(18\text{-cr})(2\text{-PrOH})_2][\{\text{Mn}(\text{acacen})_2\{\text{Fe}(\text{CN})_6\}]$ (18-cr = 18-Crown-6-ether, acacen = N,N'-ethylenebis(acetylacetonylideneiminato)). *Inorg. Chem.* **1998**, *37*, 4878–4883. [[CrossRef](#)] [[PubMed](#)]
28. Kou, H.-Z.; Ni, Z.-H.; Zhou, B.C.; Wang, R.-J. A cyano-bridged molecule-based magnet containing manganese(III) Schiff base and octacyanotungstate(V) building blocks. *Inorg. Chem. Commun.* **2004**, *7*, 1150–1153. [[CrossRef](#)]
29. Miyasaka, H.; Matsumoto, N.; Okawa, H.; Re, N.; Gallo, E.; Floriani, C. The 2-dimensional network structure and metamagnetic properties of the 2:1 complex of $[\text{Mn}(3\text{-MeOsalen})(\text{H}_2\text{O})]\text{ClO}_4$ and $\text{K}_3[\text{Fe}(\text{CN})_6]$. *Angew. Chem. Int. Ed. Engl.* **1995**, *34*, 1446–1448. [[CrossRef](#)]
30. Miyasaka, H.; Matsumoto, N.; Okawa, H.; Re, N.; Gallo, E.; Floriani, C. Complexes derived from the reaction of manganese(III) Schiff base complexes and hexacyanoferrate(III): Syntheses, multidimensional network structures, and magnetic properties. *J. Am. Chem. Soc.* **1996**, *118*, 981–994. [[CrossRef](#)]
31. Miyasaka, H.; Matsumoto, N.; Re, N.; Gallo, E.; Floriani, C. Synthesis, crystal structure, and magnetic properties of a ferrimagnetic layered compound $\text{NEt}_4[\text{Mn}(5\text{Clsalen})_2[\text{Fe}(\text{CN})_6]]$, NEt_4 = tetraethylammonium, 5-Cl-salen = N,N'-ethylenebis((5-chlorosalicylidene)aminato). *Inorg. Chem.* **1997**, *36*, 670–676. [[CrossRef](#)]
32. Miyasaka, H.; Ieda, H.; Matsumoto, N.; Sugiura, K.; Yamashita, M. Structure and magnetic properties of the two-dimensional ferrimagnet $(\text{NEt}_4)[\{\text{Mn}(\text{salen})_2\text{Fe}(\text{CN})_6\}]$: Investigation of magnetic anisotropy on a single crystal. *Inorg. Chem.* **2003**, *42*, 3509–3515. [[CrossRef](#)] [[PubMed](#)]
33. Zhou, H.-B.; Wang, J.; Wang, H.-S.; Xu, Y.-L.; Song, X.-J.; Song, Y.; You, X.-Z. Synthesis, structure, and magnetic properties of three 1D chain complexes based on high-spin metal–cyanide clusters: $[\text{Mn}^{\text{III}}_6\text{M}^{\text{III}}]$ (M = Cr, Fe, Co). *Inorg. Chem.* **2011**, *50*, 6868–6877. [[CrossRef](#)] [[PubMed](#)]

34. Pinkowicz, D.; Southerland, H.I.; Avendaño, C.; Prosvirin, A.; Sanders, C.; Wernsdorfer, W.; Pedersen, K.S.; Dreiser, J.; Clérac, R.; Nehr Korn, J.; et al. Cyanide single-molecule magnets exhibiting solvent dependent reversible “on” and “off” exchange bias behavior. *J. Am. Chem. Soc.* **2015**, *137*, 14406–14422. [CrossRef] [PubMed]
35. Sukhikh, T.S.; Vostrikova, K.E. *CSD Communication 2017, CCDC 1566469*; the Cambridge Structural Database. Available online: <http://www.ccdc.cam.ac.uk/products/csd/> (accessed on 3 August 2017). [CrossRef]
36. Sukhikh, T.S.; Vostrikova, K.E. *CSD Communication 2017, CCDC 1566470*; the Cambridge Structural Database. Available online: <http://www.ccdc.cam.ac.uk/products/csd/> (accessed on 3 August 2017). [CrossRef]
37. Sukhikh, T.S.; Vostrikova, K.E. *CSD Communication 2017, CCDC 1567014*; the Cambridge Structural Database. Available online: <http://www.ccdc.cam.ac.uk/products/csd/> (accessed on 5 August 2017). [CrossRef]
38. Sukhikh, T.S.; Vostrikova, K.E. *CSD Communication 2017, CCDC 1567013*; the Cambridge Structural Database. Available online: <http://www.ccdc.cam.ac.uk/products/csd/> (accessed on 5 August 2017). [CrossRef]
39. Zhang, W.-X.; Breedlove, B.; Ishikawa, R.; Yamashita, M. Single-chain magnets: Beyond the Glauber model. *RSC Adv.* **2013**, *3*, 3772–3798. [CrossRef]
40. Miyasaka, H.; Madanbashi, T.; Saitoh, A.; Motokawa, N.; Ishikawa, R.; Yamashita, M.; Bahr, S.; Wernsdorfer, W.; Clérac, R. Cyano-Bridged $Mn^{III}M^{III}$ Single-Chain Magnets with $M^{III} = Co^{III}, Fe^{III}, Mn^{III}$, and Cr^{III} . *Chem. Eur. J.* **2012**, *18*, 3942–3954. [CrossRef] [PubMed]
41. Przychodzeń, P.; Lewiński, K.; Bałanda, M.; Pełka, R.; Rams, M.; Wasiutyński, T.; Guyard-Duhayon, C.; Sieklucka, B. Crystal structures and magnetic properties of two low-dimensional materials constructed from $[Mn^{III}(\text{salen})H_2O]^+$ and $[M(\text{CN})_8]^{3-}/4-$ ($M = Mo$ or W) Precursors. *Inorg. Chem.* **2004**, *43*, 2967–2974. [CrossRef] [PubMed]
42. Kani, Y.; Ohba, S.; Yu, N. μ -Acetato-O:O'-bis{[bis(salicylidene)ethylenediaminato]manganese(III)} perchlorate. *Acta Cryst. C Cryst. Str. Comm.* **2000**, *56*, e194. [CrossRef] [PubMed]
43. Dolomanov, O.V.; Bourhis, L.J.; Gildea, R.J.; Howard, J.A.K.; Puschmann, H. Olex2: A complete structure solution, refinement and analysis program. *J. Appl. Cryst.* **2009**, *42*, 339–341. [CrossRef]
44. Muetterties, E.L.; Guggenberger, L.J. Idealized polytopal forms. Description of real molecules referenced to idealized polygons or polyhedra in geometric reaction path form. *J. Am. Chem. Soc.* **1974**, *96*, 1748–1756. [CrossRef]
45. Dreyer, E.B.; Lam, C.T.; Lippard, S.J. Higher coordinate cyanide and isocyanide complexes. 8. Synthesis and structure of diiododicarbonyltris(tert-butyl isocyanide)tungsten(II), an example of the 4:3 piano stool seven-coordinate geometry. *Inorg. Chem.* **1979**, *18*, 1904–1908. [CrossRef]
46. Shen, X.; Li, B.; Zou, J.; Xu, Z.; Yu, Y.; Liu, S. Crystal structure of a cyanide-bridged heptanuclear manganese(III)–chromium(III) complex with a ground state $S = 21/2$. *Trans. Met. Chem.* **2002**, *27*, 372–376. [CrossRef]
47. Shen, X.; Li, B.; Zou, J.; Hu, H.; Xu, Z. The first cyano-bridged heptanuclear $Mn(III)_6Fe(III)$ cluster: Crystal structure and magnetic properties of $[\{Mn(\text{salen})H_2O\}_6Fe(\text{CN})_6][Fe(\text{CN})_6] \cdot 6H_2O$. *J. Mol. Struct.* **2003**, *657*, 325–331. [CrossRef]
48. Nastase, S.; Maxim, C.; Duhayon, C.; Sutter, J.-P.; Andruh, M. Synthesis and crystal structure of two new cyanidobridged $[Mn^{III}_5Mo^{IV}]$ and $[Mn^{III}_2Au^I]$ heterometallic complexes. *Rev. Roum. Chim.* **2013**, *58*, 355–363.
49. Martínez, D.; Motevallia, M.; Watkinson, M. Is there really a diagnostically useful relationship between the carbon–oxygen stretching frequencies in metal carboxylate complexes and their coordination mode? *Dalton Trans.* **2010**, *39*, 446–455. [CrossRef] [PubMed]
50. SADABS, Version 2.11; Bruker Advanced X-ray Solutions: Madison, WI, USA, 2004.
51. Sheldrick, G.M. A short history of SHELX. *Acta Cryst. A* **2008**, *64*, 112–122. [CrossRef] [PubMed]

